Data Repository

Lin, S., Xing, G., Davis, D.W., Yin, C., Wu, M., Li, L., Jiang, Y., and Chen, Z., 2018, Appalachian-style multi-terrane Wilson cycle model for assembly of South China: Geology, DOI:10.1130/G39806.1

This Data Repository contains:

Figure and table numbers in the Data Repository are preceded with "DR" (e.g., Fig. DR1), to be differentiated from those in the paper.

List of Figures:

List of Tables:

1. U-Pb GEOCHRONOLOGY

1.1. Method

The samples were processed in China to concentrate zircon. Zircon samples were embedded in a polished epoxy mount (Geological Survey of Canada or GSC mount IP573) and imaged by backscattered electron microscope (BSE) and cathodoluminescence (CL). The BSE images were used to select areas for analysis, preferentially targeting primary, uniform crystal domains and avoiding cracks and alteration. The CL images were used to better reveal the zircon internal structures and to aid age interpretations.

The zircon was analyzed for U-Pb isotopes by Sensitive High Resolution Ion Microprobe (SHRIMP) at the GSC in Ottawa. A primary ion beam diameter of about 20 microns (K120 Kohler aperture) was used for all grains with analysis times of about 20 minutes per spot. Analytical procedures are described in Stern (1997). Data processing used SQUID software by Ludwig (2001).

1.2. Results and Age Interpretations

Results from 13 samples are reported here. Samples are numbered A to M in this paper for simplicity. Their corresponding field numbers (e.g., 09WY-1-1A) and GSC lab numbers (e.g. GSC 10340) are also given in this Data Repository.

Sample locations and ages are shown on Fig. 3 and their coordinates are given in Table DR1. Selected field photos of sampled units are given in Fig. DR1. Selected CL and BSE images of analyzed zircon grains are given in Fig. DR2, with the approximate locations of analytical spots outlined. Analytical data are given in Table DR1. Data are plotted on concordia diagrams (Fig. DR3) with 2 sigma error ellipses. Age errors in the text are given at 2 sigma or 95% confidence levels. Regressions were carried out using the Isoplot program of Ludwig (1982).

Sample A
09WY-1-1A (GSC 10340)
Biotite gneiss leucosome, Dajinsha "Formation", Mayuan Complex

Zircon is abundant, consisting generally of short euhedral prisms, sizes ranging from 200 to 250 μm. CL images (Fig. DR2-A) reveal oscillatory zoning in many grains but some have zoned cores with uniform overgrowths (grain 15 and 19).

Ten analyses on 9 grains gave four scattered older ages from 740-1010 Ma and a tight cluster of 6 younger data with an average $^{206}Pb/^{238}U$ age of 440 ± 4 Ma (MSWD=1.1; Fig. DR3-A). This is the best age estimate for partial melting of the gneiss. There is no clear difference between older and younger grains in CL images, except in the case of grain 19 where the core is 942 Ma but the overgrowth is 439 Ma.

Sample B
09WY-1-1B (GSC 10341)
Biotite gneiss melanosome, Dajinsha "Formation", Mayuan Complex

This sample also yielded abundant zircon with a morphology similar to sample A but relatively smaller sizes around 150 μm. CL images (Fig. DR2-B) show generally less regular oscillatory zoning due to irregular partial recrystallization of the zircon.

Ten analyses show that most of the grains cluster around 900 Ma with 2 giving younger Neoproterozoic ages (Fig. DR3-B). A subset of 6 overlapping data, in most cases from unrecrystallized zones, gives an average $^{206}Pb/^{238}U$ age of 907 ± 10 Ma. This is the best age estimate for crystallization of the protolith.

Five grains with patchy zoning were analysed on dark structureless (n.1) and bright zoned (n.2) areas on CL images. The dark areas appear to be replacing the bright ones and are usually around the rims of crystals (Fig. DR2-B, grains. 1, 3, 18). The dark areas are in all cases higher in U than the corresponding bright areas and significantly lower in Th so that their Th/U ratios are much lower. They also generally show lower Y and higher Hf. These results are consistent with metamorphic recrystallization (Pidgeon et al., 1998). In spite of the large changes in trace element chemistry, the dark areas give only moderately younger $^{206}Pb/^{238}U$ ages and in some cases are almost the same age. Either metamorphic recrystallization at 440 Ma redistributed both U and Pb within grains in equal proportions or there was an earlier metamorphism only slightly younger than the magmatic age that partly recrystallized the grains. The latter conclusion is considered to be likely since Pb should not diffuse at the same rate as U (Cherniak and Watson, 2003).

Sample C
09WY-1-2 (GSC 10342)
Pegmatite dyke intruded into Dajinsha "Formation", Mayuan Complex

This sample yielded a moderate amount of zircon, generally consisting of cracked but clear fragments with low-order faces. Their sizes are generally around 150 μm. CL images (Fig. DR2-C) show that all the grains are zoned, in some cases with bright amorphous alteration following high-U zones. There is possible minor evidence for metamorphic recrystallization (e.g. grains 8 and 17).

Ten results cluster within error with an average $^{206}Pb/^{238}U$ age of 441 ± 3 Ma (MSWD=1.0, n=9; Fig. DR3-C). This is the best age estimate for emplacement of the pegmatite.

Sample D
09WY-3-2 (GSC 10343)
Biotite gneiss, Nanshan "Formation", Mayuan Complex

Zircon from this sample is abundant, consisting of clear, stubby, multifaceted or rounded grains varying in size from 100 to 150 μm. Many grains show frosted surfaces, which may result from detrital transport. Some grains are featureless in CL images while many others show core-rim texture with regular-zoned cores surrounded by overgrowths such as grains 3 and 12 (Fig. DR2-D).

Eight analyses produced data with a range of Proterozoic ages (Fig. DR3-D) but the two youngest spots gave overlapping $^{206}Pb/^{238}U$ ages of 446 ± 6 Ma. Both the young spots were from a single overgrowth surrounding an 800 Ma old core (grain 3). Both analyses show high U but very little Th, so the overgrowth phase is likely metamorphic and may represent the remobilization age of the gneiss, which probably has a sedimentary protolith. The older Proterozoic ages ranging from 1065 Ma to 801Ma are either magmatic or metamorphic in origin, representing various ages of the source rocks.

Sample E

09WY-7-1 (GSC 10344)
Biotite gabbro

This sample yielded a population of clear-brown, stubby, multi-facetted zircon. Grains are somewhat cracked but fresh, and sizes vary from 150 to 250 μm. CL images (Fig. DR2-E) show broad zonation with no significant evidence of cores, overgrowths or metamorphic recrystallization.

Ten analyses on these igneous zonations give a concordant and tight cluster with a precise concordia age of 446 ± 4 Ma (MSWD=1.6, n=10; Fig. DR3-E).

Sample F
09WY-9-1 (GSC 10345)
Two-mica granite

Only a few dozen small stubby to long prismatic zircon grains were recovered from this sample. The grains are relatively small (around 100 μm). CL images show that most grains have regular oscillatory zonation with/without thin overgrowths (Fig. DR2-F. Analyses on 17 grains overlap well and give a concordia age of 440 ± 2 Ma (MSWD=1.0, n=17; Fig. DR3-F). This is likely the age of crystallization of the granite.

Sample G
09WY-10-1 (GSC 10346)
Metamorphosed fine-grained felsic layers in Dajinsha "Formation", Mayuan Complex

Zircon is moderately abundant and is around 150-200 μm in size. They are mostly highly cracked brown stubby grains with a small proportion of clear grains. CL images (Fig. DR2-G) also show two grain types: high-U cracked dark grains sometimes with lower U overgrowths (e.g. grains 9 and 16) and lower U almost featureless bright grains with thin overgrowths (e.g. grains 1 and 12).

Ten analyses concentrated on the cracked population show that most of the data are clustered around 930 Ma (Fig. DR3-G). This cluster may be divided into two subgroups corresponding to each grain type. Five spots on low-U clear grains give an average $^{206}Pb/^{238}U$ age of 922 ± 15 Ma. Four spots on high-U, high-Y grains give an average $^{206}Pb/^{238}U$ age of 950 ± 9 Ma, which may be due to bias of the sample-standard calibration by matrix effects. There is no distinction between Pb-Pb ages, which average to 911 ± 7 Ma (MSWD= 0.7, n= 8; Fig. DR3-G). All of the Neoproterozoic grains show Th/U ratios in the range of magmatic zircon (Th/U ratio>0.1). One datum, from an overgrowth on grain 16 gives a much younger $^{206}Pb/^{238}U$ age of 450 ± 10 Ma and a Th/U ratio near 0, suggesting that the overgrowth formed during metamorphism. Therefore, the felsic layers were probably deposited or emplaced at about 911 Ma and metamorphosed at about 450 Ma.

Sample H
09WY-11-2 (GSC 10347)
Quartz diorite

Zircon is abundant in this sample and grain sizes from 100 to 300 μm, consisting of brown-clear fragments with cracks and alteration. CL images show patchy zonation and traces of recrystallization and alteration (Fig. DR2-H).

12 data give a tightly clustered concordant data set with a concordia age of 447 ± 4 Ma (MSWD=1.4, n=12; Fig. DR3-H). This is the best estimate for crystallization of the quartz diorite.

Sample I
09WY-18-1 (GSC 10349)
Monzonite gneiss, Xiaochuan intrusion

Zircon is very abundant in this sample consisting of fresh, clear, stubby, subrounded grains sizing from 120-230 μm. Many grains show a patchy zonation under CL (Fig. DR2-I), sometimes with thin overgrowths (e.g. grain 3), whereas some grains show regular oscillatory zoning with/without recrystallization (e.g. grains 9 and 22).

Data from 13 grains show a collinear cluster with one datum showing a $^{206}Pb/^{238}U$ age of 236 ± 6 Ma and most others defining an upper concordia intercept of 1867± 7 Ma (MSWD=1.8, n=12; Fig. DR3-I). The youngest age comes from a high-U overgrowth (grain 7). Patchy bright and dark domains were dated separately, such as spots on grains 9 and 11, respectively. These spots are quite different in chemistry with much higher U and lower Th/U in the dark domains but their ages are almost identical. Spot 3.2 is from a thin overgrowth around a patchy high-U grain and shows much lower Th/U with a slightly reset age. Spot 11.2 is from a residual bright domain that appears to have been partly replaced by a high-U metamorphic domain, measured by 11.1, although the ages are again similar and slightly reset. As with sample B above, if metamorphic recrystallization occurred at 236 Ma, it would have had to redistribute both U and Pb within grains in equal proportions, which seems unlikely given the higher diffusivity of Pb relative to U (Cherniak, 2002). The alternative is that the recrystallization textures are the result of an earlier metamorphism only slightly younger than the magmatic age, or a magmatic cooling feature (Pidgeon et al., 1998).

Sample J
09WY-18-2A (GSC 10350)
Migmatite leucosome, Xiaochuan intrusion

The zircon population from this sample is similar to that from sample I. CL images also show a patchy/oscillatory zonation and overgrowths in some grains, as well as some cores (Fig. DR2-J).

12 analyses show a widely dispersed but approximately collinear pattern with an upper intercept age of 1874 ± 13 Ma and a younger concordant cluster (MSWD=2.9; Fig. DR3-J). The young cluster scatters slightly outside of error (MSWD =3.0) and gives an average $^{206}Pb/^{238}U$ age of 238 ± 3 Ma (n=9). This is the best estimate for partial melting in the migmatite. In this case, all the young data show Th/U<0.1 but the older data show higher Th/U within the range of

magmatic zircon. In general, the younger component forms featureless or zoned overgrowths around Proterozoic grains with patchy or oscillatory zonation (Fig. DR2-J).

Sample K
09WY-19-1 (GSC 10352)
Felsic metavolcanic rock, Daling Formation

This sample yielded only a few dozen small, equant, subrounded zircon grains (120-180 μm). CL images show patchy/oscillatory-zoned cores with featureless/zoned overgrowths (Fig. DR2-K).

15 analyses were performed on 11 grains. The data lie in two clusters, one a short linear distribution in the Mesoproterozoic and the other at a Permian age (Fig. DR3-K). Regression of all the data intersects concordia at 1856 ± 10 Ma and 236 ± 8 Ma but the data scatter slightly outside of error (MSWD =3.8, n=15). In general, the Mesoproterozoic data are from whole grains or cores that show patchy/oscillatory zonation while the Permian ages are from zoned overgrowths or recrystallized domains. The Mesoproterozoic ages may reflect the timing of felsic volcanism. As observed with other samples, dark patches show significantly higher U, much lower Th/U (<0.1) and lower Y than corresponding bright patches (grains 2 and 14). They probably result from metamorphic recrystallization.

The Permian phase shows very low Th/U(<0.1) and low Y, indicating that it is probably metamorphic zircon. The data are all concordant (Fig. DR3-K) but scatter along concordia significantly outside of error (MSWD =8.4, n=6). The average $^{206}Pb/^{238}U$ age is 236 ± 7 Ma. This is the best estimate of the age of metamorphism.

Sample L
09WY-22-2 (GSC 10353)
Porphyritic granite, Peizhong intrusion

Zircon is moderately abundant, consisting of small stubby and prismatic euhedral grains (100-150 μm). CL images indicate that most grains have good zonation of igneous origin and many grains have thin metamorphic overgrowths that are too narrow (less than 20 μm) to date on the SHRIMP (Fig. DR2-L).

Data on 16 grains overlap within error and give a concordia age of 403.5 ± 2.2 Ma (MSWD=1.0, n=16; Fig. DR3-L). This is probably the emplacement age of the pluton.

Sample M
Lin08-28 (GSC 9783)
Amphibolite, Zhoutan "Formation"

Zircon from this sample is moderately abundant. Grains are generally stubby or prismatic subhedral with sizes around 50-100 μm in diameter. CL images show that most zircons have patchy zonation or featureless texture (Fig. DR2-M).

Eleven analyses were performed. Six analyses overlap concordia and give overlapping $^{206}Pb/^{238}U$ ages with an average of 441 +/- 7 Ma (MSWD - 1.0) (Fig. DR3-M). Two concordant analyses (in grey on the concordia plot) are slightly younger and may have suffered secondary Pb loss so these are omitted. Three other analyses are slightly to the right of concordia, which may be an indication of either inheritance or an uncorrected common Pb component. Regressing all nine analyses gives an imprecise upper concordia intercept age of 5500 Ma, which suggests a common Pb component, and a lower intercept age of 443 +/- 10 Ma (MSWD = 1.5). Analyses from this sample show unusually high levels of common Pb (ca. 5% correction on ^{206}Pb for two of the anomalous data) possibly from uncomplete removal of the gold coating. Therefore, the most conservative estimate of age is from the regression, 443 +/- 10 Ma.

2. Lu-Hf ISOTOPES

2.1. Method

In situ zircon Lu-Hf analyses were performed using a Neptune MC-ICP-MS equipped with a 193-nmArF-excimer laser at the Institute of Geology and Geophysics, Chinese Academy of Sciences (IGGCAS) in Beijing, China. Analytical procedures were described in more detail by Wu et al. (2006). During the whole analyses, a laser beam of 44μm in diameter with a repetition rate of 8 Hz was adopted. Standard Zircons GJ-1 and Mud Tank were used as reference standards. Repeated measurements on GJ-1 and Mud Tank yielded weighted mean $^{176}Hf/^{177}Hf$ ratios of 0.282008 ± 5 (2σ, n = 43, MSWD = 2.3) and 0.282504 ± 3 (2σ, n = 43, MSWD = 1.6), respectively, which are in good agreement with the recommended values within 2σ error (Morel et al., 2008; Sláma et al., 2008; Xie et al., 2008). Calculation of εHf(t) values was based on the present chondritic uniform reservoir (CHUR) values with $^{176}Hf/^{177}Hf$ = 0.282785 and $^{176}Lu/^{177}Hf$ = 0.0336 (Bouvier et al., 2008), using the decay constant of ^{176}Lu of 1.867 10-11 yr-1 (Söderlund et al., 2004). Two-stage depleted mantle model (T_{DM2}) ages were adopted in this study and calculated with a mean $^{176}Lu/^{177}Hf$ ratio of 0.015 for the average continental crust (Amelin et al., 1999). All the zircon Lu-Hf isotopic data and calculation details are presented in Table DR2 with an error of 2σ.

2.2. Summary of Results

As shown on the εHf(t) values versus zircon formation age diagram (Fig. 4), zircons from all samples preserved variable Hf isotopic compositions against relatively consistent formation ages. Magmatic zircons from East Cathaysia have εHf(t) values varying from -5.5 to +8.0 with T_{DM2} ages clustering between 3.0 and 2.4 Ga. In contrast, magmatic zircons from the West Cathaysia show variable εHf(t) values from -10.0 to +4.4 with T_{DM2} ages clustering between 2.2 and 1.5 Ga. For the metamorphic zircons, as Lu-Hf isotopic system is generally considered to be resistant to the modification of metamorphism (Kinny and Maas, 2003; Wu et al., 2007; Zeh et al., 2010), we assume the metamorphic zircons inherited the primary Hf signatures from the magmatic zircons.

3. SOURCES OF DATA COMPILED IN FIGURES 1, 2, 3 AND 4

Figure 1: 261 (± 1) Ma is a LA-ICP-MS age of metamorphic zircon from a marble from Zhoushan Islands, Zhejiang Province (Yang et al., 2016). 1832 (± 13) Ma is a SHRIMP age of igneous zircon from an amphibolite (meta-tonalite) from a drill hole in East China Sea (Xing G.F., unpublished data).

Figure 2: The Hf histograms are based on data from:
For the Jiuling terrane: Yin et al. (2013), and Wang W. et al. (2013)
For the Shuangxiwu Group: Chen et al. (2009), and Li et al. (2009)
For the Tieshajie Formation: Li et al. (2013)
For West Cathaysia: from Fig. 5.
For East Cathaysia: from Fig. 5.

Figure 3: U-Pb ages shown in black are compiled from Li et al. (1994), Chen et al. (1998), Chen et al. (2008), Li et al. (2008), Li et al. (2010), Li et al. (2013), Liu et al. (2010), Wan et al. (2007), Xia et al. (2012), Wang et al. (2012, 2014), Wang Y.J. (2013), Yu et al. (2009), and Zhao et al. (2014, 2015).

Figure 4: Hf data shown in grey are compiled from:
For West Cathaysia: Yu et al. (2005), Zeng et al. (2008), Liu et al. (2010), Wang D. et al. (2013)
For East Cathaysia: Xiang et al. (2008), Yu et al. (2009), Xia et al. (2012), Zhao et al. (2014, 2015)

4. PHOTOS OF MYLONITE FROM NORTHWEST FUJIAN FAULT

See Figure DR4 (p. 22)

5. SCHEMATIC DIAGRAM SHOWING THE TECTONIC EVOLUTION OF THE EASTERN MARGIN OF NORTH AMERICA, WITH FOCUS ON THE APPALACHIAN OROGEN

See Figure DR5 (p. 23)

REFERENCES

Amelin, Y., Lee, D.-C., Halliday, A. N., and Pidgeon, R. T., 1999, Nature of the Earth's earliest crust from hafnium isotopes in single detrital zircons: Nature, v. 399, no. 6733, p. 252-255.

Bouvier, A., Vervoort, J. D., and Patchett, P. J., 2008, The Lu–Hf and Sm–Nd isotopic composition of CHUR: Constraints from unequilibrated chondrites and implications for the bulk composition of terrestrial planets: Earth and Planetary Science Letters, v. 273, no. 1–2, p. 48-57.

Chen, D.F., Li, X.H., Pan, J.M., Dong, W.Q., Chen, G.Q., Chen, X.P., 1998. Metamorphic newly produced zircons, SHRIMP Ion microprobe U–Pb age of the amphibolite of Hexi Group,

Zhejiang and its implications. ActaMinerologica Sinica 4, 396–400 (in Chinese with English abstract).
Chen, C.-H., Lee, C.-Y., Hsieh, P.-S., Zeng, W., and Zhou, H.-W., 2008, Approaching the age problem for some metamorphosed Precambrian basement rocks and Phanerozoic granitic bodies in the Wuyishan area: The application of EMP monazite age dating: Geological Journal of China Universities, v. 14, no. 1, p. 1–15.
Chen, Z., Xing, G., Guo, K., Dong, Y., Chen, R., Zeng, Y., Li, L., He. Z., and Zhao, L., 2009, Petrogenesis of keratophyes in the Pingshui Group, Zhejiang: Constraints from zircon U-Pb ages and Hf isotopes: Chinese Science Bulletin, v54, p. 1570-1578.
Cherniak, D.J. and Watson, E.B., 2003, Diffusion in zircon. *in* Reviews in Mineralogy and Geochemistry, J.M. Hanchar and P.W.O. Hoskin (eds.), v. 53, Mineralogical Society of America, Washington, DC, pp 113–143.
Jaffey, A.H., Flynn, K.F., Glendenin, L.E., Bentley, W.C., and Essling, A.M., 1971, Precision measurement of half-lives and specific activities of 235U and 238U. Physical Review 4: p. 1889-1906.
Jiang, Y, Xing, G.F, Yuan, Q, Zhao, X.L, Duan, Z, Dong, X.F., 2016, The first discovery of Permian metamorphic rocks in Zhoushan Islands, Zhejiang Province. Geological Bulletin of China, v. 35, p. 1046-1055 (in Chinese with English abstract).
Kinny, P. D., and Maas, R., 2003, Lu–Hf and Sm–Nd isotope systems in zircon: Reviews in Mineralogy and Geochemistry, v. 53, no. 1, p. 327-341.
Li, X.-H., Zhou, G.Q., Zhao, J., Fanning, C.M., Compston, W., 1994, SHRIMP ion probe zircon age of the NE Jiangxi ophiolite and its tectonic implications. Geochimica 23, 117–123 (in Chinese with English abstarct).
Li, W.X., Li, X.H., Li, Z.X., and Lou, F.S., 2008, Obduction-type granites within the NE Jiangxi Ophiolite: Implications for the final amalgamation between the Yangtze and Cathaysia Blocks: Gondwana Research, v. 13, p. 288–301.
Li, X.-H., Li, W.-X., Li, Z.-X., Lo, C.-H., Wang, J., Ye, M.-F., and Yang, Y.-H., 2009, Amalgamation between the Yangtze and Cathaysia Blocks in South China: Constraints from SHRIMP U–Pb zircon ages, geochemistry and Nd–Hf isotopes of the Shuangxiwu volcanic rocks: Precambrian Research, v. 174, no. 1–2, p. 117-128.
Li, Z.X., Li, X.H.,Wartho, J.A., Clark, C., Li,W.X., Zhang, C.L., and Bao, C.M., 2010, Magmatic and metamorphic events during the early Paleozoic Wuyi-Yunkai orogeny, southeastern South China: New age constraints and pressure–temperature conditions. Geological Society of America Bulletin, v.122, p. 772–793.
Li, L., Lin, S., Xing, G., Davis, D.W., Davis, W.J., Xiao, W., and Yin, C., 2013, Geochemistry and tectonic implications of late Mesoproterozoic alkaline bimodal volcanic rocks from the Tieshajie Group in the southeastern Yangtze Block, South China. Precambrian Research, v. 230, p. 179–192.
Liu, R., Zhou, H., Zhang, L., Zhong, Z., Zeng, W., Xiang, H., Jin, S., Lu, X., and Li, C., 2010, Zircon U–Pb ages and Hf isotope compositions of the Mayuan migmatite complex, NW Fujian Province, Southeast China: Constraints on the timing and nature of a regional tectonothermal event associated with the Caledonian orogeny: Lithos, v. 119, no. 3–4, p. 163-180.
Ludwig, K.R., 2003, User's manual for Isoplot 3.00 a geochronological toolkit for Excel. Berkeley Geochronological Center Special Publication 4, 71 p. (www.bgc.org/isoplot_etc/Isoplot3betaManual.pdf)

Ludwig, K.R., 2001, User's manual for Squid 1.02. Berkeley Geochronological Center Special Publication 2, 19 pp.(www.bgc.org/isoplot_etc/Squid1.03Manual.pdf)
Marshak, S., 2008, Earth: Portrait of a Planet (3rd Edition). W.W. Norton & Company, 832 p.
Morel, M. L. A., Nebel, O., Nebel-Jacobsen, Y. J., Miller, J. S., and Vroon, P. Z., 2008, Hafnium isotope characterization of the GJ-1 zircon reference material by solution and laser-ablation MC-ICPMS: Chemical Geology, v. 255, no. 1–2, p. 231-235.
Pidgeon, R.T., Nemchin, A.A., and Hitchen, G.J., 1998, Internal structures of zircons from Archaean granites from the Darling Range batholith: implications for zircon stability and the interpretation of zircon U-Pb ages. Contributions to Mineralogy and Petrology, v. 132, p. 288-299.
Sláma, J., Košler, J., Condon, D. J., Crowley, J. L., Gerdes, A., Hanchar, J. M., Horstwood, M. S. A., Morris, G. A., Nasdala, L., Norberg, N., Schaltegger, U., Schoene, B., Tubrett, M. N., and Whitehouse, M. J., 2008, Plešovice zircon — A new natural reference material for U–Pb and Hf isotopic microanalysis: Chemical Geology, v. 249, no. 1–2, p. 1-35.
Söderlund, U., Patchett, P. J., Vervoort, J. D., and Isachsen, C. E., 2004, The ^{176}Lu decay constant determined by Lu–Hf and U–Pb isotope systematics of Precambrian mafic intrusions: Earth and Planetary Science Letters, v. 219, no. 3–4, p. 311-324.
van Staal, C.R., Whalen, J.B., Valverde-Vaquero, P., Zagorevski, A., and Rogers, N., 2009, Pre-Carboniferous, episodic accretion-related, orogenesis along the Laurentian margin of the northern Appalachians, *in* Murphy, J.B., Keppie, J.D., and Hynes, A.J., eds., Ancient orogens and modern analogues: London, Geological Society [London] Special Publication 327, p. 271-316.
Wan, Y., Liu, D., Xu, M., Zhuang, J., Song, B., Shi, Y., and Du, L., 2007, SHRIMP U-Pb zircon geochronology and geochemistry of metavolcanic and metasedimentary rocks in northwestern Fujian, Cathaysia block, China: Tectonic implications and the need to redefine lithostratigraphic units: Gondwana Research, v. 12, no. 1–2, p. 166–183
Wang, D., Zheng, J., Ma, Q., Griffin, W. L., Zhao, H., and Wong, J., 2013, Early Paleozoic crustal anatexis in the intraplate Wuyi–Yunkai orogen, South China: Lithos, v. 175–176, p. 124-145.
Wang, W., Zhou, M.-F., Yan, D.-P., Li, L., and Malpas, J., 2013, Detrital zircon record of Neoproterozoic active-margin sedimentation in the eastern Jiangnan Orogen, South China: Precambrian Research, v. 235, p. 1-19.
Wang, Y.J., Wu, C.M., Zhang, A.M., Fan, W.M., Zhang, Y.H., Zhang, Y.Z., Peng, T.P., Yin, C.Q., 2012. Kwangsian and Indosinian reworking of the eastern South China Block: constraints on zircon U–Pb geochronology and metamorphism of amphibolite and granulite. Lithos, v. 150, p. 227–242.
Wang, Y.J., Zhang, A.M., Cawood, P.A., Zhang, Y.Z., Fan, W.M., and Zhang, G.W., 2013, Geochronological and geochemical fingerprinting of an early Neoproterozoic arc-back-arc system in South China and its accretionary assembly along the margin of Rodinia: Precambrian Research, v. 231, p. 343-371.
Wang, Y.J., Zhang, Y.Z., Fan, W.M., Geng, H.Y., Zoua H.P., Bi, X.W., 2014, Early Neoproterozoic accretionary assemblage in the Cathaysia Block:Geochronological, Lu–Hf isotopic and geochemical evidence from granitoid gneisses. Precambrian Research 249, 144–161

Wu, F.-Y., Yang, Y.-H., Xie, L.-W., Yang, J.-H., and Xu, P., 2006, Hf isotopic compositions of the standard zircons and baddeleyites used in U–Pb geochronology: Chemical Geology, v. 234, no. 1–2, p. 105-126.

Wu, Y. B., Zheng, Y. F., Zhang, S. B., Zhao, Z. F., Wu, F. Y., and Liu, X. M., 2007, Zircon U–Pb ages and Hf isotope compositions of migmatite from the North Dabie terrane in China: constraints on partial melting: Journal of Metamorphic Geology, v. 25, no. 9, p. 991-1009.

Stern, R. A. 1997. The GSC sensitive high ion microprobe (SHRIMP): analytical techniques of zircon U-Th-Pb age determinations and performance evaluation. Geological Survey of Canada – Current Research, pp. 1-31.

Xia, Y., Xu, X.-S., and Zhu, K.-Y., 2012, Paleoproterozoic S- and A-type granites in southwestern Zhejiang: Magmatism, metamorphism and implications for the crustal evolution of the Cathaysia basement: Precambrian Research, v. 216–219, p. 177-207.

Xiang, H., Zhang, L., Zhou, H., Zhong, Z., Zeng, W., Liu, R., and Jin, S., 2008, U-Pb zircon geochronology and Hf isotope study of metamorphosed basic-ultrabasic rocks from metamorphic basement in southwestern Zhejiang: The response of the Cathaysia Block to Indosinian orogenic event: Science in China Series D: Earth Sciences, v. 51, no. 6, p. 788.

Xie, L., Zhang, Y., Zhang, H., Sun, J., and Wu, F., 2008, In situ simultaneous determination of trace elements, U-Pb and Lu-Hf isotopes in zircon and baddeleyite: Chinese Science Bulletin, v. 53, no. 10, p. 1565-1573.

Yin, C.Q., Lin, S., Davis, D.W., Xing, G.F., Davis, W.J., Cheng, G.H., Xiao, W.J., and Li, L.M., 2013, Tectonic evolution of the southeastern margin of the Yangtze Block: Constraints from SHRIMP U-Pb and LA-ICP-MS Hf isotopic studies of zircon from the eastern Jiangnan Orogenic Belt and implications for the tectonic interpretation of South China: Precambrian Research, v. 236, p. 145–156.

Yu, J., Zhou, X., O'Reilly, Y. S., Zhao, L., Griffin, W. L., Wang, R., Wang, L., and Chen, X., 2005, Formation history and protolith characteristics of granulite facies metamorphic rock in Central Cathaysia deduced from U-Pb and Lu-Hf isotopic studies of single zircon grains: Chinese Science Bulletin, v. 50, no. 18, p. 2080-2089.

Yu, J.-H., Wang, L., O'Reilly, S. Y., Griffin, W. L., Zhang, M., Li, C., and Shu, L., 2009, A Paleoproterozoic orogeny recorded in a long-lived cratonic remnant (Wuyishan terrane), eastern Cathaysia Block, China: Precambrian Research, v. 174, no. 3–4, p. 347-363.

Zeh, A., Gerdes, A., Will, T. M., and Frimmel, H. E., 2010, Hafnium isotope homogenization during metamorphic zircon growth in amphibolite-facies rocks: Examples from the Shackleton Range (Antarctica): Geochimica et Cosmochimica Acta, v. 74, no. 16, p. 4740-4758.

Zeng, W., Zhang, L., Zhou, H., Zhong, Z., Xiang, H., Liu, R., Jin, S., Lü, X., and Li, C., 2008, Caledonian reworking of Paleoproterozoic basement in the Cathaysia Block: Constraints from zircon U-Pb dating, Hf isotopes and trace elements: Chinese Science Bulletin, v. 53, no. 6, p. 895-904.

Zhao, L., Zhou, X., Zhai, M., Santosh, M., Ma, X., Shan, H., and Cui, X., 2014, Paleoproterozoic tectonic transition from collision to extension in the eastern Cathaysia Block, South China: Evidence from geochemistry, zircon U–Pb geochronology and Nd–Hf isotopes of a granite–charnockite suite in southwestern Zhejiang: Lithos, v. 184–187, p. 259-280.

Zhao, L., Zhou, X., Zhai, M., Santosh, M., and Geng, Y., 2015, Zircon U–Th–Pb–Hf isotopes of the basement rocks in northeastern Cathaysia block, South China: Implications for

Phanerozoic multiple metamorphic reworking of a Paleoproterozoic terrane: Gondwana Research, v. 28, no. 1, p. 246-261.

Fig. DR1: Selected field photos of igneous and metamorphic rocks sampled for SHRIMP U-Pb geochronology. Corresponding sample numbers are indicated on the photos. Samples A & B: Biotite gneiss, Mayuan complex. Sample C: Pegmatite dyke in the Mayuan complex. Sample E: Biotite gabbro, with pegmatitic patches. Sample F: Two mica granite, Zhuzhou intrusion. Sample J: orthogneiss, Xiaochuan intrusion. Sample M: Amphibolite, Zhoutan Formation

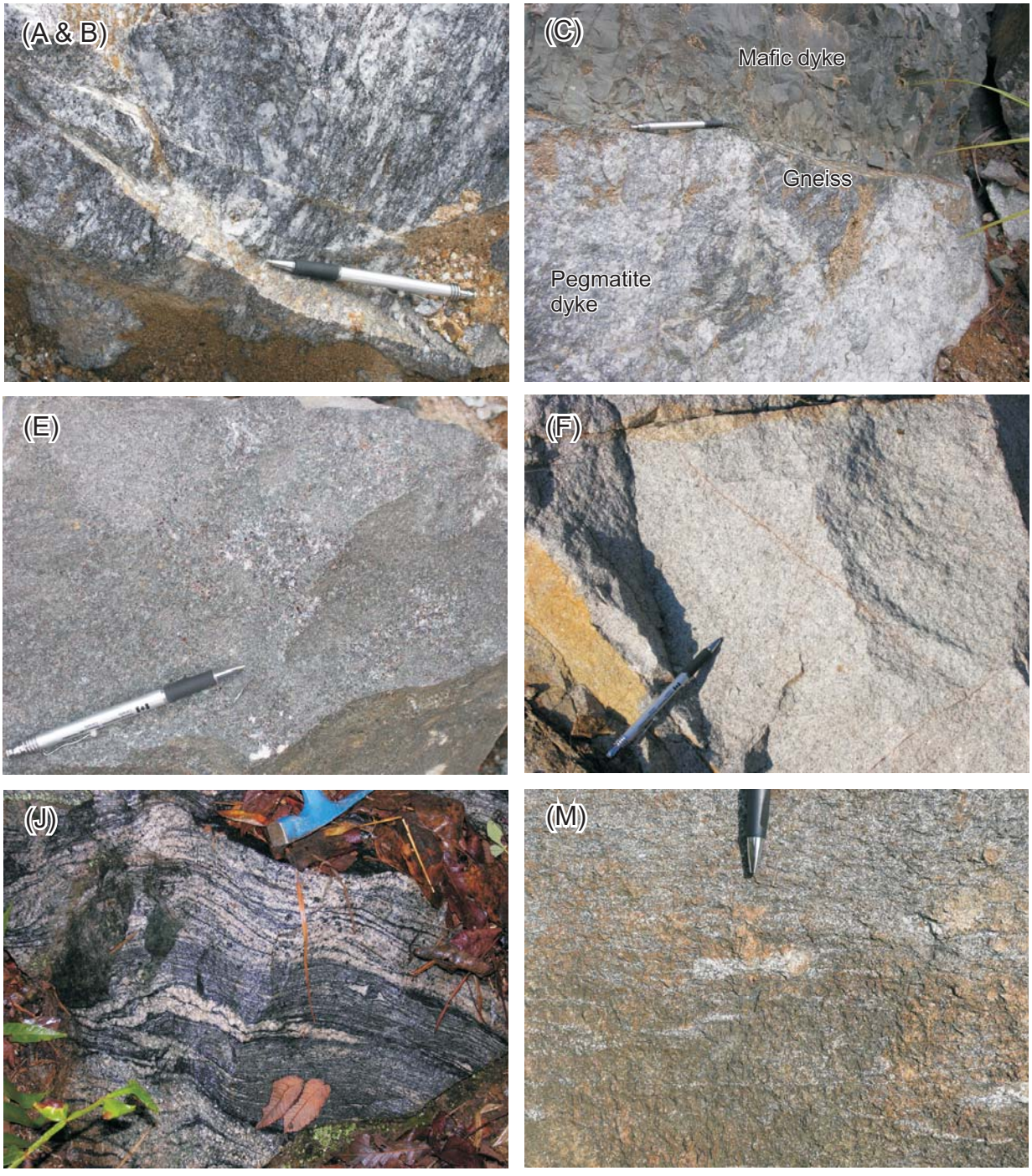

Fig. DR2. Selected CL and BSE images of dated zircon grains (samples A-C)

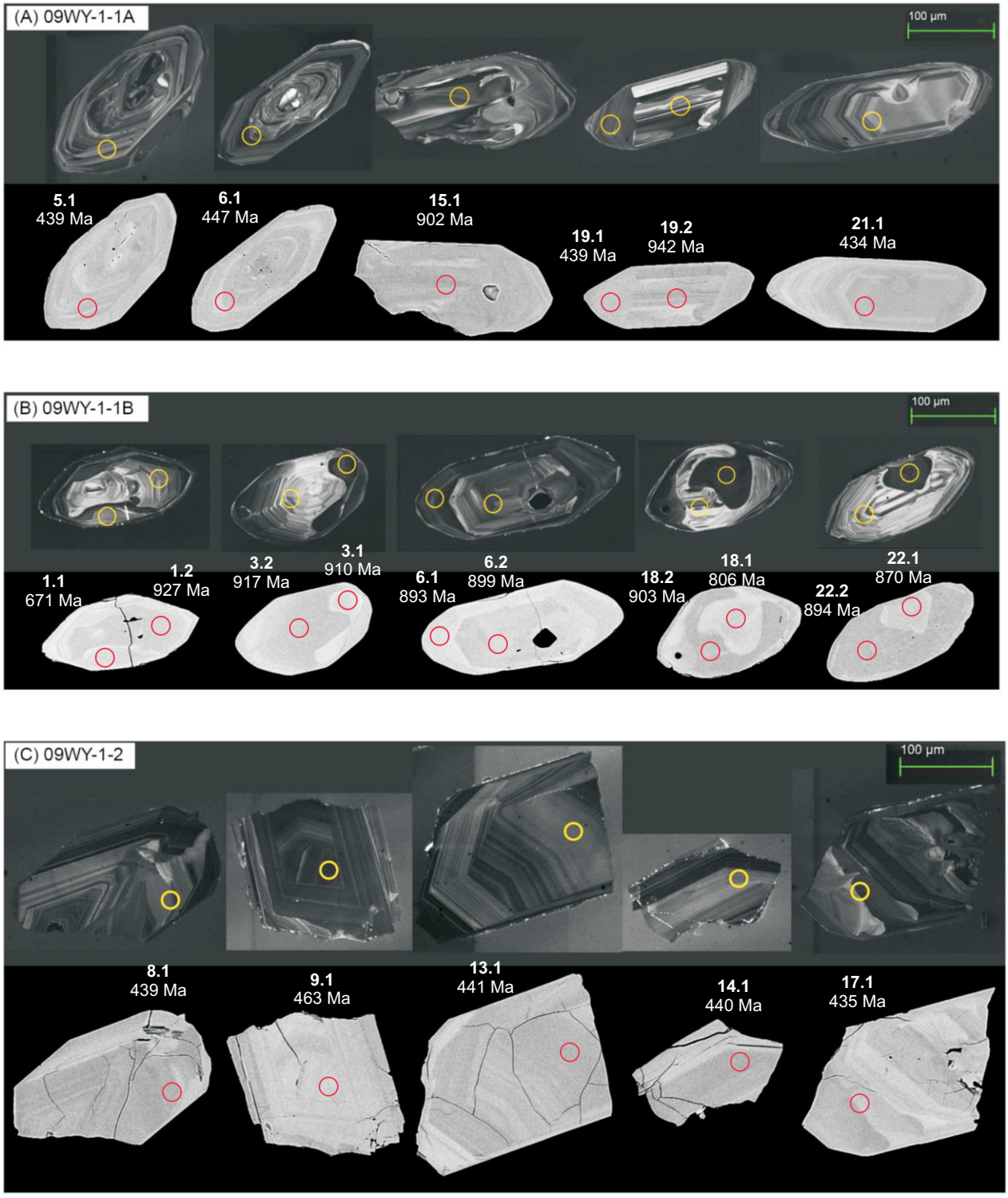

Fig. DR2. Selected CL and BSE images of dated zircon grains (samples D-F)

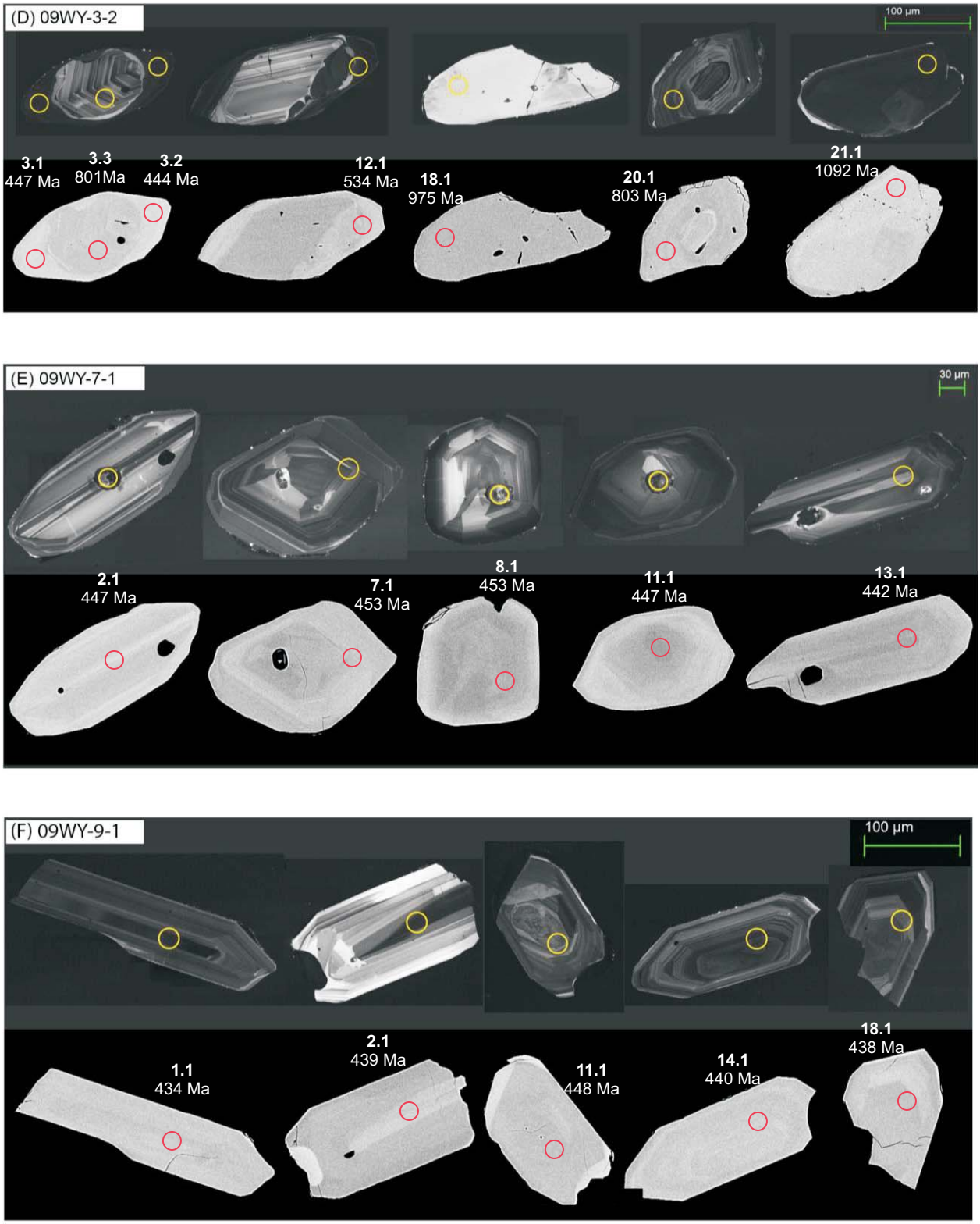

Fig. DR2. Selected CL and BSE images of dated zircon grains (samples G-I)

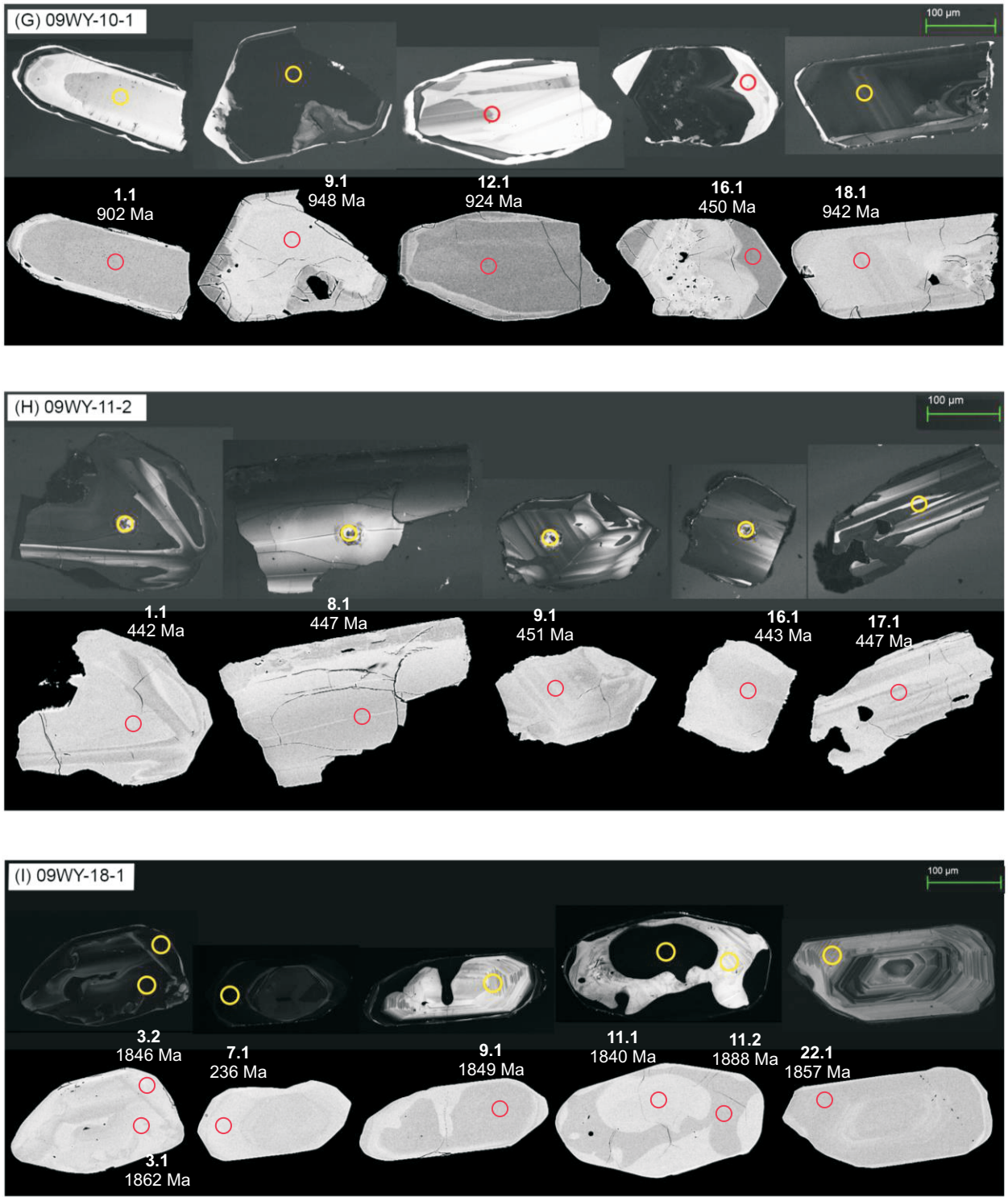

Fig. DR2. Selected CL and BSE images of dated zircon grains (samples J-L)

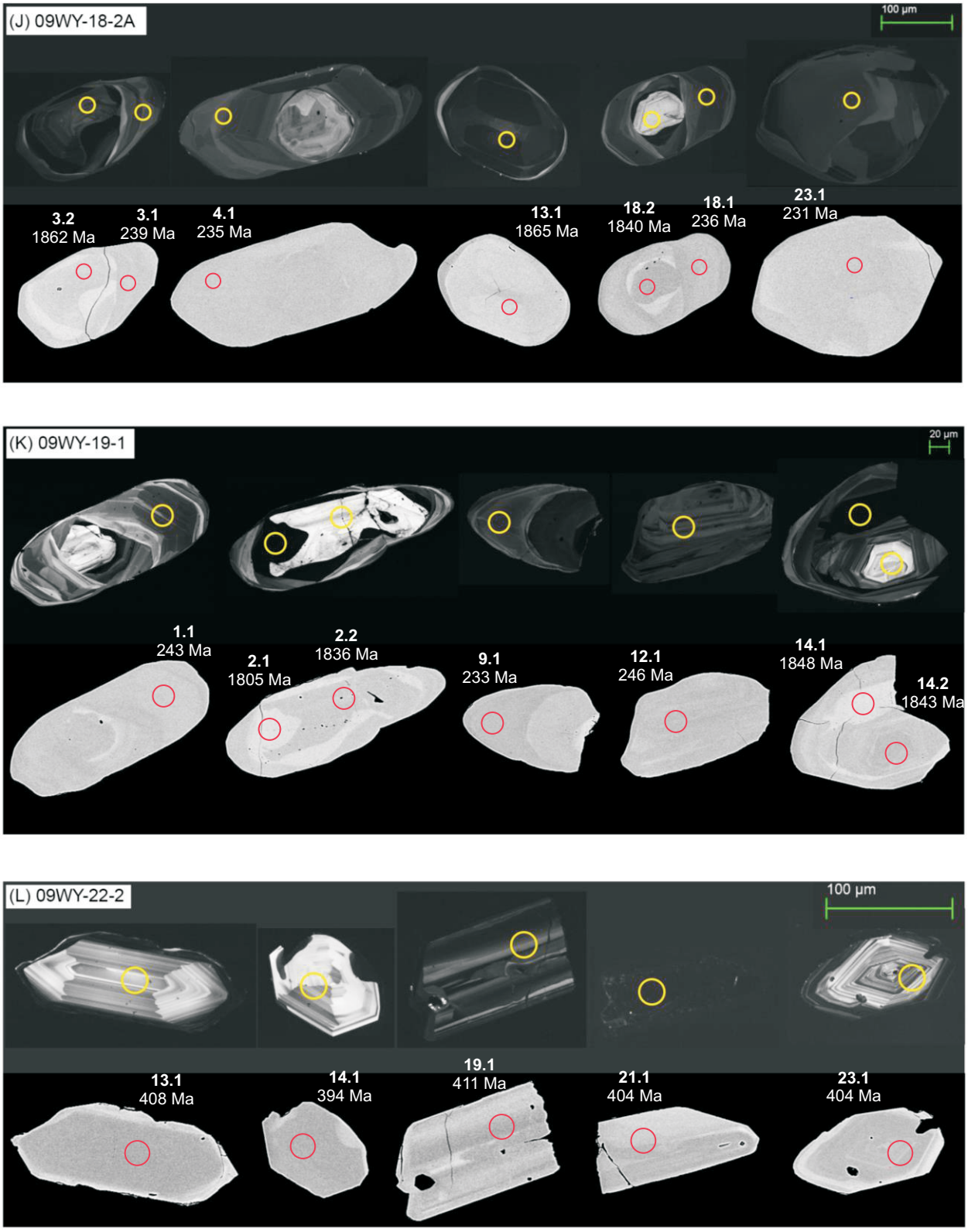

Fig. DR2. Selected CL and BSE images of dated zircon grains (sample M)

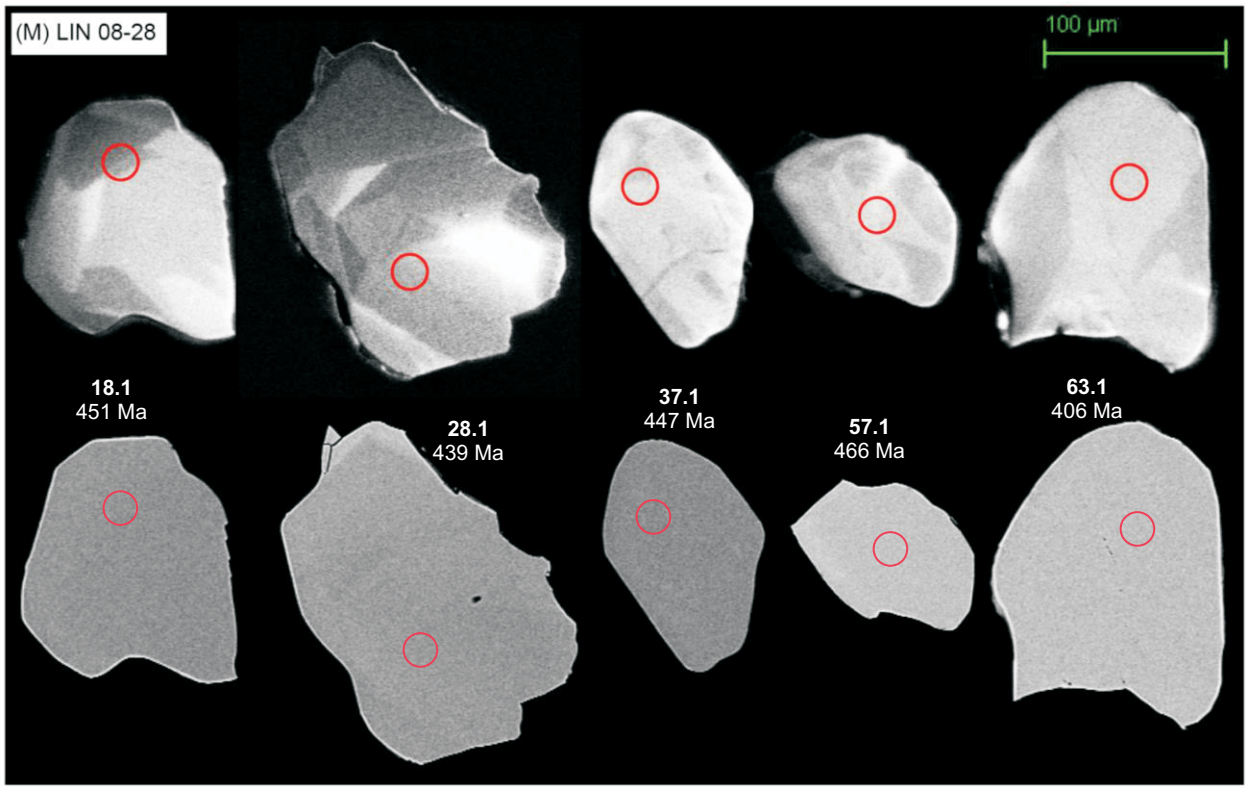

Fig. DR3, Concordia diagrams (samples A-D)

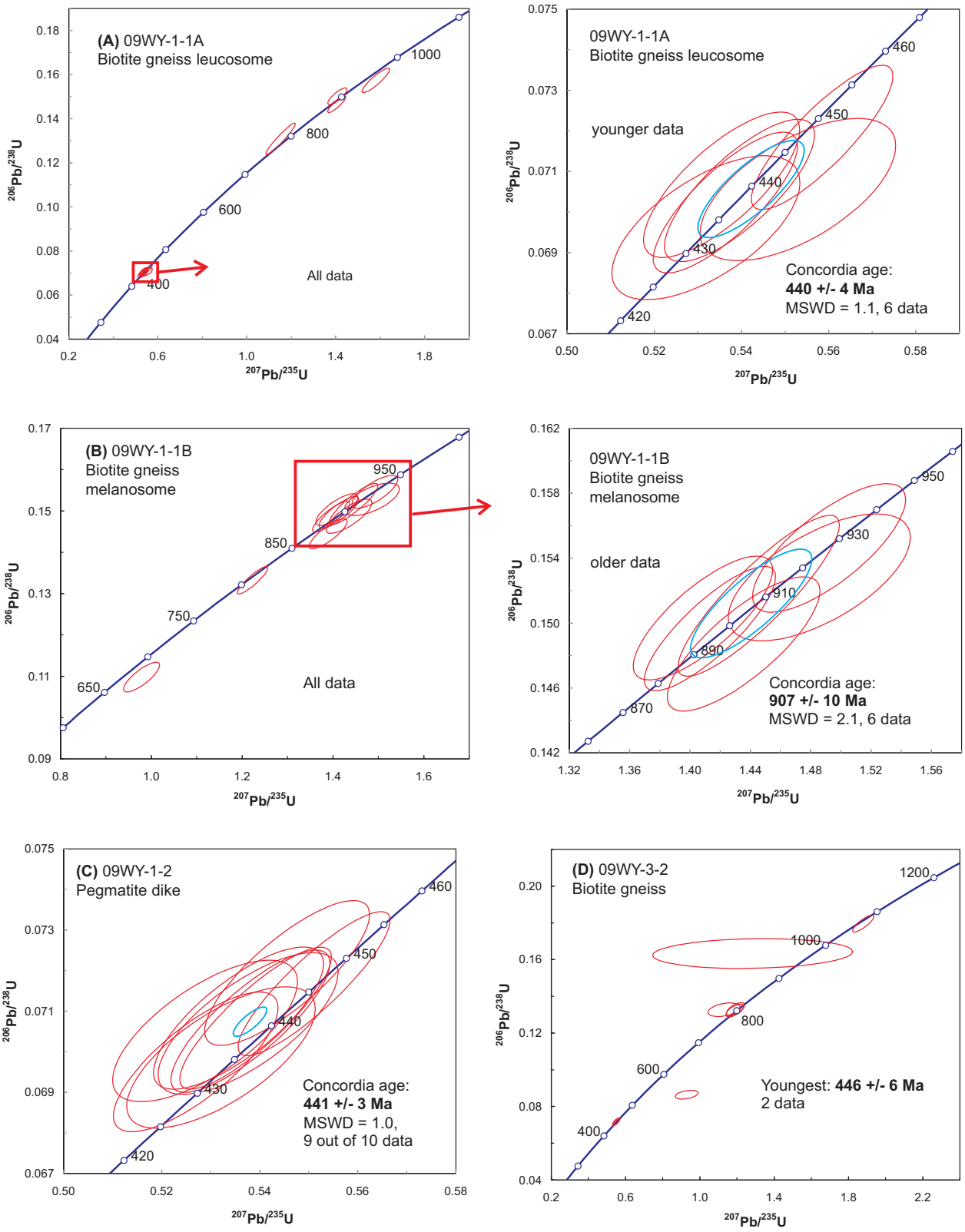

Fig. DR3, Concordia diagrams (samples E-I)

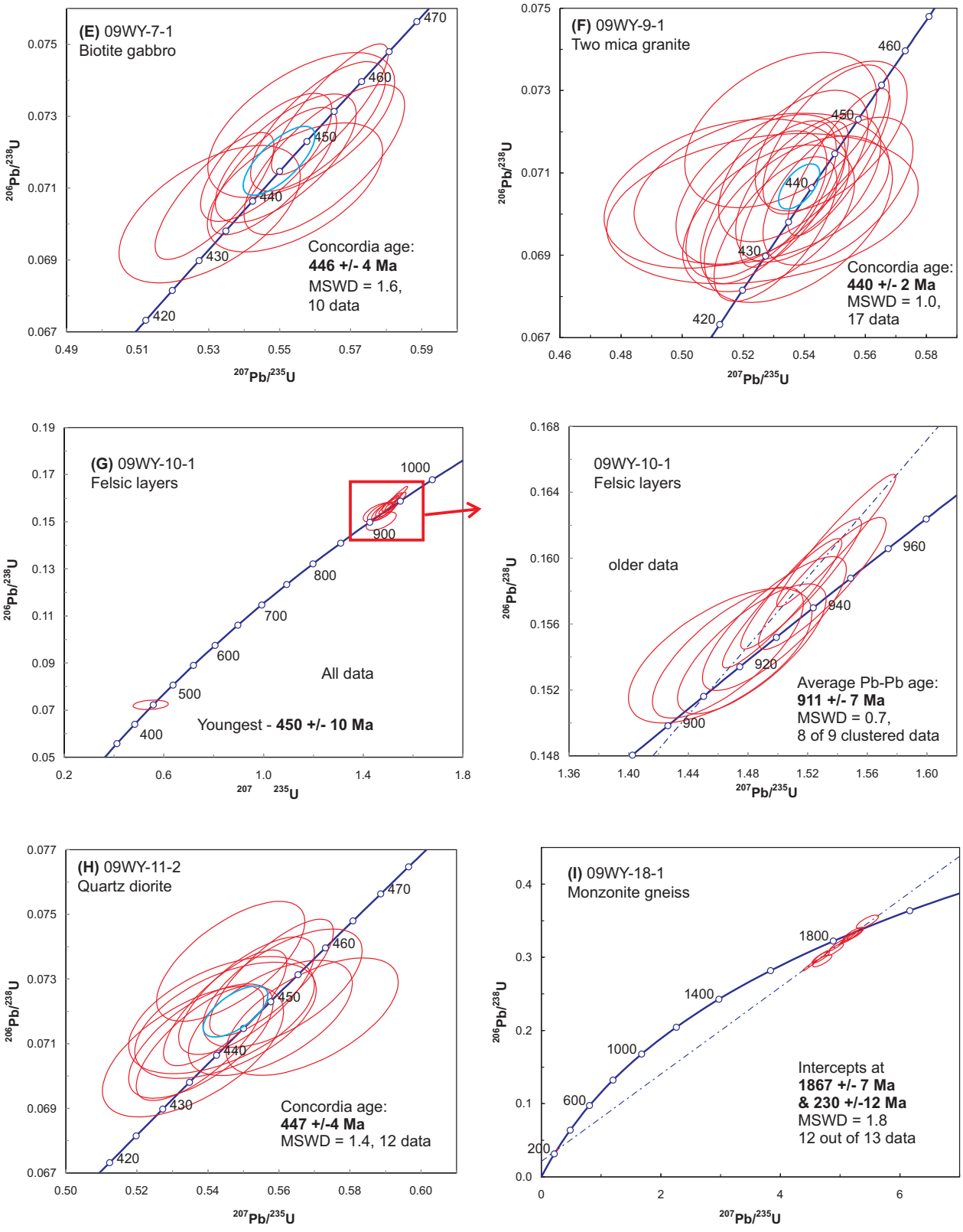

Fig. DR3. Concordia diagrams (samples J-M)

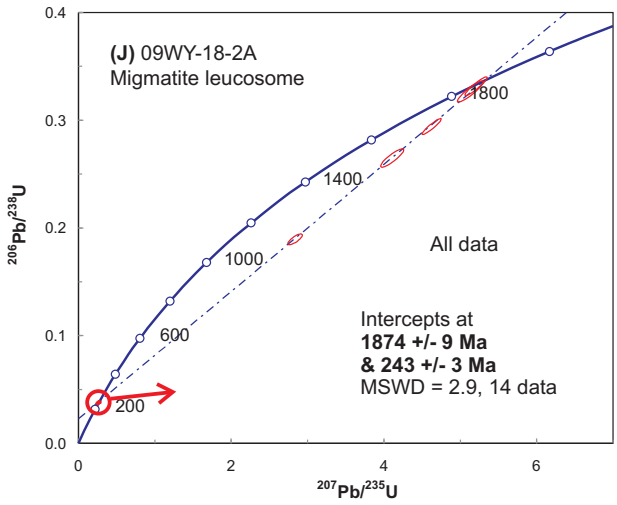

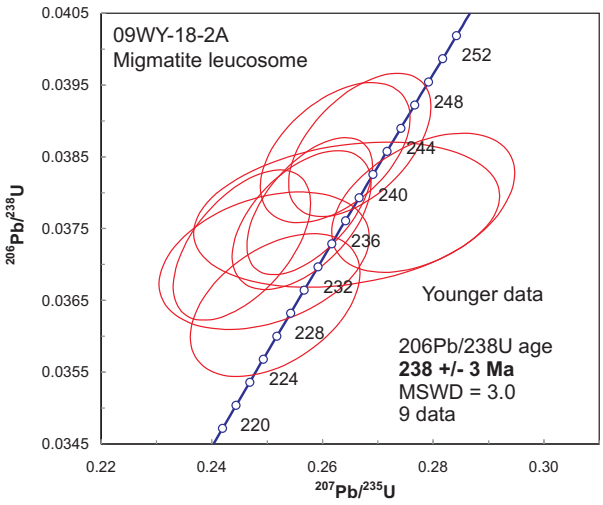

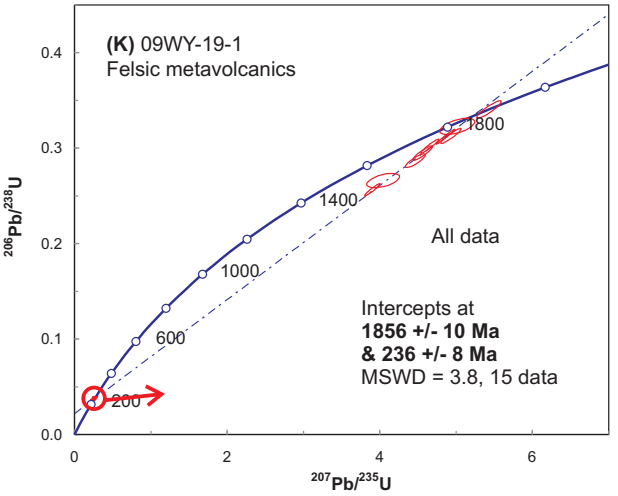

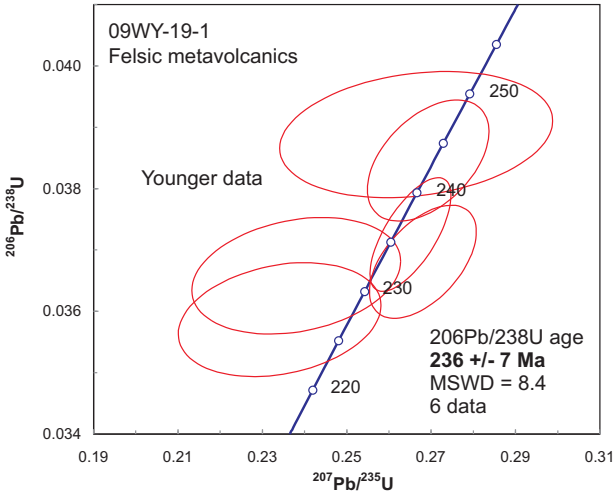

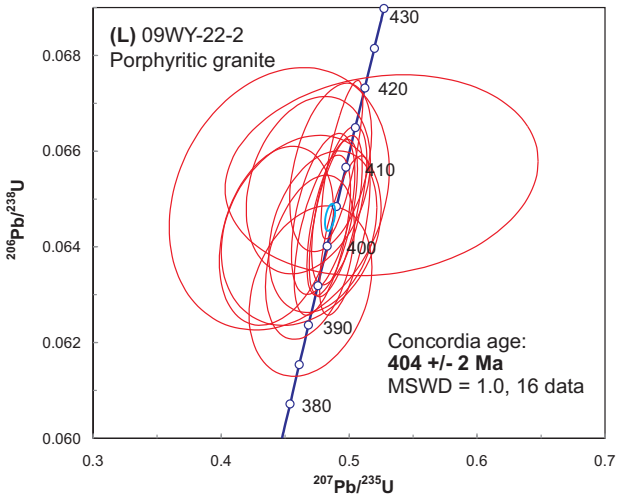

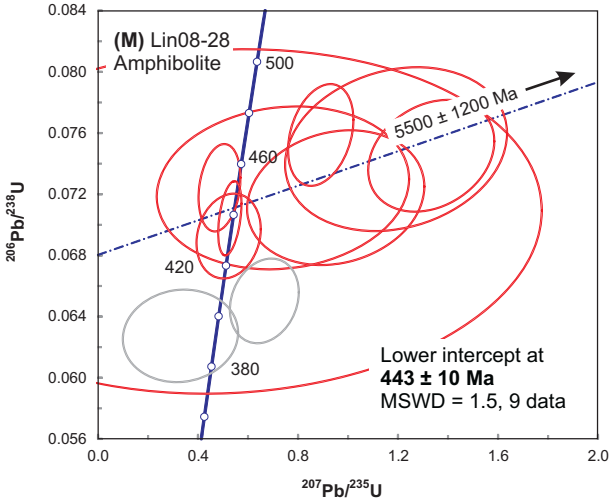

Fig. DR4: Highly deformed rocks (mylonites) from the Northwest Fujian Fault. All surfaces shown are subhorizontal, subparallel to stretching lineations.

(A) Field photo. Note the highly deformed and boudinaged quartz veins. The "S"-shaped drag folds are consistent with sinistral shear.

(B) A mylonite sample and sketch showing both sinistral and dextral shear bands. Note that a dextral shear band overprints a sinistral one.

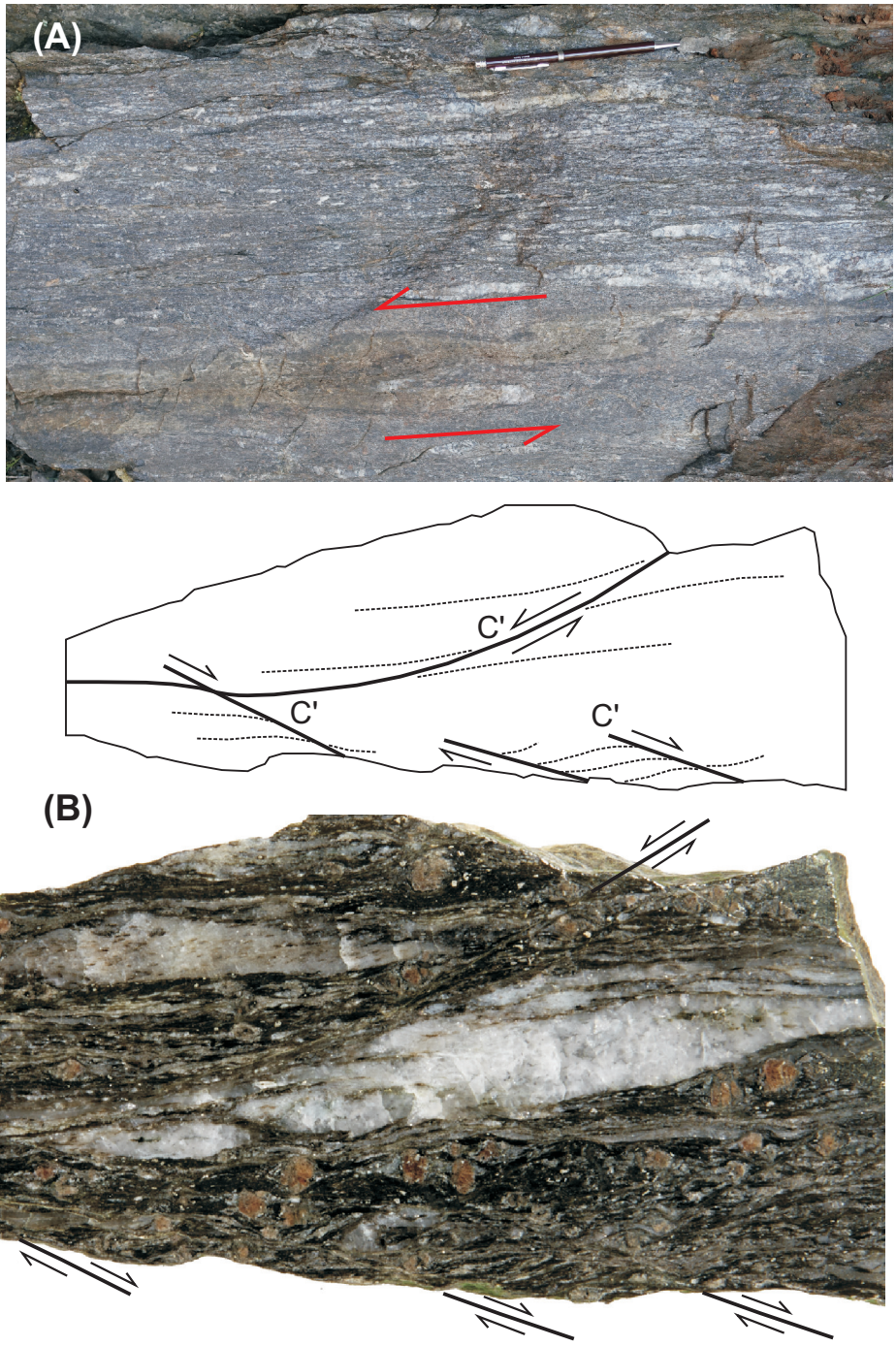

Fig. DR5: Schematic diagram showing a simplified version of the tectonic evolution of the eastern margin of North America, based on the Appalachian orogen in the U.S. (modified after figure 11.39 of Marshak, 2008). In the Appalachian orogen, multiple terranes, including arcs and (micro)continents of both Laurentian and Gondwanan origin, accreted to the eastern margin of Laurentia during the Taconic (Ordovician), Salinic (Silurian; not shown here), Acadian (Devonian) and Alleghanian (Carboniferous) orogenies . Both the Amazonian and African continents that collided with North America during the ~1.0 Ga Grenvillian and the Carboniferous Alleghanian orogeny, respectively, rifted away from Laurentia after each collision, leading to the opening of the Iapetus and Atlantic oceans, respectively.

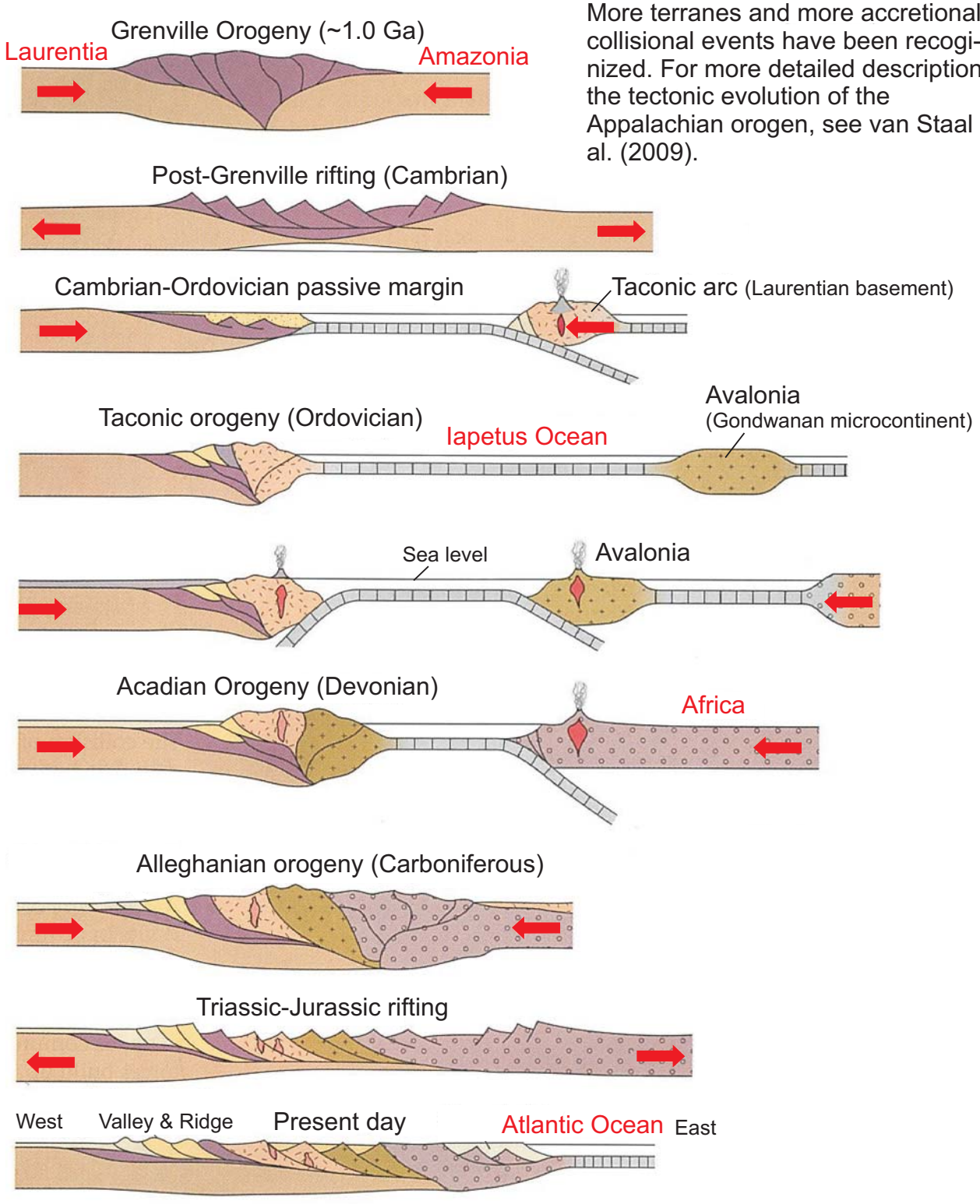

More terranes and more accretional/ collisional events have been recognized. For more detailed description of the tectonic evolution of the Appalachian orogen, see van Staal et al. (2009).

Table DR2: Zircon Lu-Hf data for samples from South China

Analysis spot	$^{176}Yb/^{177}Hf$	2σ	$^{176}Lu/^{177}Hf$	2σ	$^{176}Hf/^{177}Hf$	2σ	U-Pb age (Ma)	$(^{176}Hf/^{177}Hf)_i$	$\varepsilon Hf_{(0)}$	$f_{Lu/hf}$	$\varepsilon Hf_{(t)}$	T_{DM1} (Ga)	$T_{DM2\ (c.c)}$ (Ga)
(A) 09WY-1-1A Biotite gneiss leucosome, Dajinsha "Formation", Mayuan Complex													
2	0.032802	0.000147	0.001131	0.000002	0.282389	0.000017	438	0.282379	-13.6	-0.97	-4.3	1.22	1.69
5	0.033202	0.000067	0.001135	0.000001	0.282378	0.000013	439	0.282368	-13.9	-0.97	-4.6	1.24	1.72
6	0.034355	0.000146	0.001135	0.000008	0.282273	0.000015	447	0.282263	-17.7	-0.97	-8.2	1.39	1.95
7	0.061915	0.000508	0.002103	0.000013	0.282222	0.000018	882	0.282187	-19.5	-0.94	-1.2	1.50	1.85
9	0.035767	0.000089	0.001235	0.000006	0.282382	0.000015	440	0.282372	-13.8	-0.96	-4.5	1.24	1.71
11	0.052522	0.000359	0.001754	0.000018	0.282239	0.000016	793	0.282213	-18.8	-0.95	-2.3	1.46	1.85
15	0.046214	0.002489	0.001529	0.000076	0.282238	0.000016	902	0.282212	-18.9	-0.95	0.1	1.45	1.78
19.1	0.020203	0.000381	0.000725	0.000014	0.282359	0.000026	439	0.282353	-14.6	-0.98	-5.1	1.25	1.75
19.2	0.086508	0.001597	0.002839	0.000044	0.282195	0.000018	942	0.282144	-20.4	-0.91	-1.4	1.57	1.90
21	0.016555	0.000060	0.000567	0.000003	0.282362	0.000014	434	0.282357	-14.5	-0.98	-5.1	1.24	1.75
(B) 09WY-1-1B Biotite gneiss melanosome, Dajinsha "Formation", Mayuan Complex													
3.1	0.030217	0.000556	0.001197	0.000022	0.282349	0.000023	910	0.282328	-15.0	-0.96	4.4	1.28	1.51
3.2	0.065801	0.000462	0.002270	0.000023	0.282173	0.000019	917	0.282134	-21.2	-0.93	-2.3	1.57	1.94
6.1	0.044803	0.000209	0.001603	0.000007	0.282226	0.000020	893	0.282199	-19.3	-0.95	-0.5	1.47	1.81
6.2	0.039976	0.000323	0.001368	0.000014	0.282222	0.000018	899	0.282199	-19.4	-0.96	-0.4	1.47	1.81
18.1	0.040804	0.001283	0.001500	0.000043	0.282206	0.000017	806	0.282183	-20.0	-0.95	-3.0	1.49	1.90
18.2	0.054867	0.000319	0.002049	0.000018	0.282186	0.000022	903	0.282151	-20.7	-0.94	-2.0	1.55	1.91
22.1	0.043473	0.000863	0.001662	0.000033	0.282184	0.000021	870	0.282157	-20.8	-0.95	-2.5	1.53	1.92
22.2	0.055191	0.000484	0.002053	0.000020	0.282267	0.000021	894	0.282232	-17.9	-0.94	0.7	1.43	1.74
(C) 09WY-1-2 Pegmatite dyke intruded into Dajinsha "Formation", Mayuan Complex													
4	0.024122	0.000320	0.000821	0.000007	0.282339	0.000013	435	0.282332	-15.3	-0.98	-6.0	1.28	1.80
7	0.044180	0.000781	0.001522	0.000024	0.282343	0.000014	441	0.282330	-15.2	-0.95	-5.9	1.30	1.80

8	0.039211	0.000257	0.001324	0.000006	0.282355	0.000012	439	0.282345	-14.7	-0.96	-5.5	1.28	1.77
9	0.112495	0.000955	0.003777	0.000016	0.282375	0.000017	463	0.282342	-14.1	-0.89	-5.0	1.34	1.76
12	0.088889	0.001476	0.002959	0.000056	0.282399	0.000013	446	0.282374	-13.2	-0.91	-4.3	1.27	1.70
13	0.055215	0.000913	0.001888	0.000036	0.282366	0.000012	441	0.282350	-14.4	-0.94	-5.2	1.28	1.76
14	0.039662	0.000863	0.001355	0.000021	0.282330	0.000013	440	0.282318	-15.6	-0.96	-6.4	1.31	1.83
17	0.030428	0.000308	0.001048	0.000008	0.282328	0.000012	435	0.282320	-15.7	-0.97	-6.4	1.31	1.83
19	0.037683	0.000091	0.001273	0.000002	0.282336	0.000012	441	0.282326	-15.4	-0.96	-6.1	1.30	1.81
22	0.034526	0.000132	0.001202	0.000001	0.282372	0.000012	448	0.282362	-14.1	-0.96	-4.6	1.25	1.73
(D) 09WY-3-2 Biotite gniess, Nanshan “Formation”, Mayuan Complex													
1	0.009699	0.000024	0.000348	0.000000	0.282193	0.000017	805	0.282188	-20.5	-0.99	-2.9	1.47	1.89
3.1	0.049535	0.000616	0.002082	0.000025	0.282135	0.000037	447	0.282118	-22.5	-0.94	-13.3	1.62	2.27
3.2	0.056122	0.000315	0.002411	0.000010	0.282120	0.000025	444	0.282100	-23.1	-0.93	-14.0	1.66	2.31
3.3	0.024260	0.000267	0.000853	0.000008	0.281897	0.000019	801	0.281884	-31.0	-0.97	-13.8	1.90	2.57
12	0.034368	0.000690	0.001405	0.000030	0.282005	0.000026	534	0.281991	-27.1	-0.96	-15.9	1.77	2.50
18	0.014613	0.000032	0.000521	0.000001	0.282236	0.000029	975	0.282226	-19.0	-0.98	2.3	1.42	1.70
20	0.015400	0.000078	0.000545	0.000002	0.282215	0.000018	803	0.282207	-19.7	-0.98	-2.3	1.44	1.85
21	0.011036	0.000086	0.000344	0.000002	0.281502	0.000017	1092	0.281495	-44.9	-0.99	-21.0	2.41	3.25
(E) 09WY-7-1 Biotite gabbro													
2	0.014765	0.000307	0.000633	0.000010	0.282208	0.000030	447	0.282202	-20.0	-0.98	-10.3	1.46	2.08
3	0.019271	0.000287	0.000841	0.000009	0.282328	0.000033	447	0.282321	-15.7	-0.97	-6.1	1.30	1.82
4	0.019434	0.000575	0.000851	0.000026	0.282281	0.000022	455	0.282273	-17.4	-0.97	-7.6	1.37	1.92
6	0.010080	0.000082	0.000425	0.000003	0.282248	0.000019	441	0.282245	-18.5	-0.99	-8.9	1.39	1.99
7	0.012609	0.000086	0.000527	0.000005	0.282257	0.000024	453	0.282253	-18.2	-0.98	-8.4	1.39	1.97
8	0.024880	0.000231	0.001009	0.000006	0.282289	0.000028	453	0.282281	-17.1	-0.97	-7.4	1.36	1.91
10	0.022183	0.000141	0.000921	0.000002	0.282325	0.000025	445	0.282317	-15.8	-0.97	-6.3	1.31	1.83
11	0.018151	0.000107	0.000766	0.000007	0.282313	0.000027	447	0.282307	-16.2	-0.98	-6.6	1.32	1.85
13	0.014721	0.000056	0.000591	0.000002	0.282260	0.000024	442	0.282255	-18.1	-0.98	-8.6	1.38	1.97
16	0.019610	0.000103	0.000766	0.000002	0.282327	0.000027	438	0.282321	-15.7	-0.98	-6.3	1.30	1.82

(F) 09WY-9-1 Two mica granite

1	0.039574	0.000309	0.001411	0.000009	0.282383	0.000020	434	0.282372	-13.8	-0.96	-4.6	1.24	1.71
2	0.026291	0.000778	0.000871	0.000022	0.282393	0.000014	439	0.282386	-13.4	-0.97	-4.0	1.21	1.68
3	0.034191	0.000611	0.001140	0.000018	0.282404	0.000015	448	0.282394	-13.0	-0.97	-3.5	1.20	1.65
4	0.045550	0.000406	0.001597	0.000008	0.282380	0.000014	444	0.282367	-13.9	-0.95	-4.6	1.25	1.72
5	0.033399	0.000052	0.001163	0.000003	0.282390	0.000017	438	0.282380	-13.5	-0.96	-4.2	1.22	1.69
9	0.034301	0.000477	0.001114	0.000014	0.282364	0.000017	440	0.282354	-14.4	-0.97	-5.1	1.26	1.75
11	0.019085	0.000384	0.000640	0.000015	0.282355	0.000015	448	0.282350	-14.7	-0.98	-5.1	1.25	1.75
12	0.026783	0.000061	0.000937	0.000002	0.282400	0.000015	439	0.282392	-13.2	-0.97	-3.8	1.20	1.66
13	0.022772	0.000622	0.000836	0.000025	0.282423	0.000024	440	0.282416	-12.4	-0.97	-2.9	1.17	1.61
14	0.027573	0.000319	0.000912	0.000008	0.282343	0.000015	440	0.282336	-15.2	-0.97	-5.8	1.28	1.79
18	0.027021	0.000496	0.000906	0.000013	0.282339	0.000017	438	0.282332	-15.3	-0.97	-5.9	1.29	1.80
19	0.031611	0.000504	0.001071	0.000020	0.282502	0.000016	436	0.282493	-9.5	-0.97	-0.3	1.06	1.44
21	0.025927	0.000176	0.000876	0.000009	0.282357	0.000014	447	0.282349	-14.7	-0.97	-5.1	1.26	1.76
22	0.025238	0.000092	0.000895	0.000003	0.282383	0.000015	437	0.282375	-13.8	-0.97	-4.4	1.22	1.70
24	0.036073	0.000415	0.001241	0.000017	0.282376	0.000013	443	0.282365	-14.0	-0.96	-4.6	1.25	1.72
26	0.014780	0.000036	0.000484	0.000002	0.282389	0.000014	435	0.282385	-13.5	-0.99	-4.1	1.20	1.68
28	0.029905	0.000267	0.001019	0.000007	0.282411	0.000015	440	0.282402	-12.8	-0.97	-3.4	1.19	1.64

(G) 09WY-10-1 Metamorphosed fine-grained felsic layers in Dajinsha "Formation", Mayuan Complex

1	0.070503	0.000447	0.002191	0.000008	0.282239	0.000023	902	0.282202	-18.8	-0.93	-0.2	1.47	1.80
7	0.041241	0.000700	0.001411	0.000027	0.282243	0.000018	935	0.282218	-18.7	-0.96	1.1	1.44	1.74
9	0.096631	0.000285	0.003171	0.000017	0.282242	0.000018	948	0.282185	-18.7	-0.90	0.2	1.51	1.81
12	0.024596	0.000212	0.000763	0.000003	0.282159	0.000019	924	0.282146	-21.7	-0.98	-1.7	1.53	1.91
13	0.017904	0.000054	0.000595	0.000001	0.282151	0.000016	925	0.282141	-22.0	-0.98	-1.9	1.53	1.92
16	0.007407	0.000362	0.000292	0.000015	0.282251	0.000016	450	0.282248	-18.4	-0.99	-8.6	1.39	1.98
18	0.047589	0.000341	0.001506	0.000003	0.282227	0.000017	942	0.282200	-19.3	-0.95	0.6	1.46	1.78
19	0.065644	0.000225	0.002249	0.000003	0.282237	0.000017	948	0.282197	-18.9	-0.93	0.6	1.48	1.78
20	0.088034	0.000281	0.002931	0.000006	0.282268	0.000018	963	0.282215	-17.8	-0.91	1.6	1.46	1.73

21	0.052052	0.002195	0.001706	0.000058	0.282194	0.000022	926	0.282164	-20.4	-0.95	-1.0	1.52	1.87
(H) 09WY-11-2 Quartz diorite													
1	0.044307	0.002529	0.001482	0.000077	0.282474	0.000019	442	0.282462	-10.5	-0.96	-1.2	1.11	1.51
2	0.010911	0.000098	0.000433	0.000004	0.282469	0.000016	449	0.282465	-10.7	-0.99	-1.0	1.09	1.49
6	0.062345	0.000215	0.002083	0.000003	0.282488	0.000020	454	0.282470	-10.0	-0.94	-0.7	1.11	1.48
8	0.062499	0.002980	0.001970	0.000090	0.282461	0.000022	447	0.282444	-11.0	-0.94	-1.7	1.15	1.54
9	0.096230	0.000313	0.003202	0.000012	0.282530	0.000020	451	0.282503	-8.6	-0.90	0.4	1.08	1.41
10	0.073345	0.000741	0.002493	0.000025	0.282516	0.000020	447	0.282495	-9.1	-0.92	0.0	1.08	1.43
11	0.055595	0.000841	0.001867	0.000032	0.282563	0.000017	447	0.282548	-7.4	-0.94	1.9	1.00	1.31
14	0.037484	0.000593	0.001278	0.000017	0.282454	0.000018	441	0.282443	-11.3	-0.96	-1.9	1.14	1.55
15	0.043532	0.001014	0.001476	0.000034	0.282490	0.000021	457	0.282478	-10.0	-0.96	-0.3	1.09	1.46
16	0.022516	0.001543	0.000763	0.000045	0.282422	0.000016	443	0.282416	-12.4	-0.98	-2.9	1.17	1.61
17	0.042200	0.001473	0.001474	0.000038	0.282487	0.000021	447	0.282475	-10.1	-0.96	-0.7	1.10	1.47
18	0.070587	0.001732	0.002416	0.000051	0.282543	0.000023	452	0.282522	-8.1	-0.93	1.1	1.04	1.36
(I) 09WY-18-1 Monzonite gneiss, Xiaochuan intrusion													
2	0.020818	0.000246	0.000659	0.000008	0.281458	0.000014	1871	0.281434	-46.5	-0.98	-5.6	2.49	2.89
3	0.030501	0.000203	0.000989	0.000008	0.281597	0.000015	1862	0.281562	-41.6	-0.97	-1.3	2.32	2.61
6	0.017655	0.000049	0.000607	0.000001	0.281493	0.000015	1875	0.281472	-45.2	-0.98	-4.2	2.43	2.81
7	0.004113	0.000048	0.000120	0.000001	0.283112	0.000016	236	0.283112	12.0	-1.00	17.2	0.19	0.16
8	0.009027	0.000128	0.000246	0.000003	0.281568	0.000014	1854	0.281559	-42.6	-0.99	-1.6	2.31	2.62
9	0.019634	0.000106	0.000641	0.000003	0.281596	0.000016	1849	0.281573	-41.6	-0.98	-1.2	2.30	2.59
10	0.034249	0.000464	0.001099	0.000013	0.281623	0.000017	1876	0.281584	-40.6	-0.97	-0.2	2.29	2.55
11	0.005103	0.000023	0.000149	0.000001	0.281520	0.000015	1888	0.281515	-44.3	-1.00	-2.3	2.37	2.70
12	0.004583	0.000011	0.000182	0.000000	0.281405	0.000016	2133	0.281398	-48.3	-0.99	-0.9	2.53	2.80
14	0.019760	0.000047	0.000678	0.000001	0.281554	0.000018	1867	0.281530	-43.1	-0.98	-2.3	2.36	2.68
22	0.024267	0.000385	0.000860	0.000016	0.281552	0.000018	1857	0.281522	-43.1	-0.97	-2.8	2.37	2.70
(J) 09WY-18-2A Migmatite leucosome, Xiaochuan intrusion													
3.1	0.001128	0.000023	0.000031	0.000001	0.282101	0.000013	239	0.282101	-23.7	-1.00	-18.5	1.58	2.43

3.2	0.039643	0.000320	0.001317	0.000007	0.281577	0.000014	1862	0.281531	-42.2	-0.96	-2.4	2.36	2.68
4	0.000358	0.000007	0.000010	0.000000	0.281954	0.000018	235	0.281954	-28.9	-1.00	-23.8	1.78	2.75
5	0.019422	0.000055	0.000657	0.000001	0.281596	0.000016	1863	0.281573	-41.6	-0.98	-0.8	2.30	2.59
8	0.000812	0.000006	0.000025	0.000000	0.281934	0.000014	245	0.281933	-29.6	-1.00	-24.3	1.81	2.79
10	0.018539	0.000112	0.000631	0.000002	0.281561	0.000019	1777	0.281539	-42.8	-0.98	-4.0	2.34	2.72
13	0.010746	0.000032	0.000310	0.000001	0.281527	0.000017	1865	0.281516	-44.0	-0.99	-2.8	2.37	2.71
14	0.000494	0.000016	0.000014	0.000000	0.281935	0.000016	240	0.281935	-29.6	-1.00	-24.3	1.80	2.79
15	0.000870	0.000007	0.000025	0.000000	0.282031	0.000015	244	0.282030	-26.2	-1.00	-20.9	1.68	2.58
18.1	0.001001	0.000008	0.000031	0.000000	0.281924	0.000016	236	0.281924	-30.0	-1.00	-24.8	1.82	2.82
18.2	0.023104	0.000115	0.000762	0.000005	0.281561	0.000014	1840	0.281534	-42.8	-0.98	-2.8	2.35	2.69
19.1	0.000645	0.000009	0.000019	0.000000	0.281951	0.000016	238	0.281951	-29.0	-1.00	-23.8	1.78	2.76
19.2	0.006598	0.000305	0.000228	0.000013	0.282246	0.000015	239	0.282245	-18.6	-0.99	-13.4	1.39	2.11
23	0.001001	0.000009	0.000027	0.000000	0.281815	0.000015	231	0.281815	-33.8	-1.00	-28.8	1.97	3.06
(K) 09WY-19-1 Felsic metavolcanics, Daling Formation													
1	0.000840	0.000006	0.000025	0.000000	0.281931	0.000013	243	0.281931	-29.7	-1.00	-24.4	1.81	2.80
2.1	0.004912	0.000053	0.000156	0.000002	0.281559	0.000016	1805	0.281554	-42.9	-1.00	-2.8	2.32	2.67
2.2	0.030686	0.000162	0.000975	0.000006	0.281600	0.000018	1836	0.281566	-41.5	-0.97	-1.7	2.31	2.62
9	0.000550	0.000007	0.000015	0.000000	0.281948	0.000015	233	0.281948	-29.1	-1.00	-24.0	1.79	2.77
11.1	0.008708	0.000389	0.000332	0.000015	0.281847	0.000036	1848	0.281836	-32.7	-0.99	8.1	1.94	2.00
12	0.003915	0.000570	0.000100	0.000014	0.281984	0.000018	246	0.281984	-27.9	-1.00	-22.5	1.74	2.68
14.1	0.005623	0.000109	0.000164	0.000002	0.281552	0.000015	1848	0.281546	-43.1	-1.00	-2.1	2.33	2.66
14.2	0.031835	0.000118	0.001041	0.000002	0.281573	0.000018	1843	0.281537	-42.4	-0.97	-2.6	2.35	2.68
17	0.035293	0.000308	0.001209	0.000014	0.281761	0.000019	1829	0.281719	-35.8	-0.96	3.6	2.10	2.28
18.1	0.001011	0.000012	0.000028	0.000000	0.281972	0.000016	236	0.281972	-28.3	-1.00	-23.1	1.75	2.71
18.2	0.001150	0.000014	0.000036	0.000000	0.282016	0.000024	227	0.282016	-26.7	-1.00	-21.8	1.70	2.62
(L) 09WY-22-2 Porphyritic granite, Peizhong intrusion													
1	0.037573	0.000744	0.001401	0.000034	0.282497	0.000022	402	0.282486	-9.7	-0.96	-1.3	1.08	1.48
3	0.015596	0.000390	0.000600	0.000014	0.282460	0.000018	401	0.282455	-11.0	-0.98	-2.4	1.11	1.55

5	0.022893	0.000313	0.000878	0.000010	0.282349	0.000031	405	0.282342	-15.0	-0.97	-6.3	1.27	1.80
6	0.026803	0.000955	0.001119	0.000030	0.282451	0.000024	402	0.282443	-11.3	-0.97	-2.8	1.14	1.57
9	0.029447	0.000280	0.001075	0.000008	0.282464	0.000020	401	0.282456	-10.9	-0.97	-2.4	1.12	1.55
10	0.039289	0.000312	0.001427	0.000014	0.282519	0.000022	399	0.282508	-8.9	-0.96	-0.6	1.05	1.43
13	0.038410	0.001149	0.001321	0.000036	0.282490	0.000022	408	0.282480	-10.0	-0.96	-1.3	1.09	1.49
14	0.030717	0.000113	0.001104	0.000004	0.282510	0.000020	394	0.282502	-9.3	-0.97	-0.9	1.05	1.45
15	0.028674	0.000217	0.001039	0.000006	0.282473	0.000024	410	0.282465	-10.6	-0.97	-1.8	1.10	1.52
19	0.054382	0.000642	0.001840	0.000019	0.282554	0.000020	411	0.282540	-7.7	-0.94	0.8	1.01	1.35
20	0.030838	0.001729	0.001102	0.000052	0.282407	0.000020	404	0.282398	-12.9	-0.97	-4.3	1.20	1.67
23	0.040727	0.000335	0.001443	0.000006	0.282503	0.000020	404	0.282492	-9.5	-0.96	-1.0	1.07	1.46
26	0.059916	0.000660	0.002136	0.000023	0.282520	0.000040	406	0.282503	-8.9	-0.94	-0.6	1.07	1.44

The formulas used are as follows: $\varepsilon Hf_{(t)} = (({}^{176}Hf/{}^{177}Hf)_S-({}^{176}Lu/{}^{177}Hf)_S\times(e^{\lambda t}-1))/(({}^{176}Hf/{}^{177}Hf)_{CHUR,0}-({}^{176}Lu/{}^{177}Hf)_{CHUR}\times(e^{\lambda t}-1))-1)\times10000$; $T_{DM1}=1/\lambda\times\ln(1+(({}^{176}Hf/{}^{177}Hf)_S-({}^{176}Hf/{}^{177}Hf)_{DM})/(({}^{176}Lu/{}^{177}Hf)_S-({}^{176}Lu/{}^{177}Hf)_{DM}))$; $T_{DM2} = T_{DM1} - (T_{DM1} - t) \times ((f_{CC} - f_S) / (f_{CC} - f_{DM}))$, where $({}^{176}Lu/{}^{177}Hf)_S$ and $({}^{176}Hf/{}^{177}Hf)_S$ are the measured values of samples; $({}^{176}Lu/{}^{177}Hf)_{CHUR} = 0.0332$ and $({}^{176}Hf/{}^{177}Hf)_{CHUR,0} = 0.282772$ (Blichert-Toft and Albarede, 1997); $({}^{176}Lu/{}^{177}Hf)_{DM} = 0.0384$ and $({}^{176}Hf/{}^{177}Hf)_{DM} = 0.28325$ (Griffin et al., 2000); f_{CC}, f_S and f_{DM} are the $f_{Lu/Hf}$ values of average continental crust, the sample and the depleted mantle, respectively; $f_{CC} = -0.55$ (Amelin et al., 1999), $f_{DM} = 0.16$ (Griffin et al., 2000); $\lambda = 1.867\times10^{-11}$/y (Söderlund et al., 2004); and t = crystallization time of zircon.